Comparison between First- and Second-Generation Praseodymium Precursors for the MOCVD Synthesis of Praseodymium Aluminate Thin Films

Raffaella Lo Nigro,*,† Roberta G. Toro,‡ Graziella Malandrino,*,‡ and Ignazio L. Fragalà‡

Istituto per la Microelettronica e Microsistemi, IMM-CNR, Stradale Primosole n 50, 95121 Catania, Italy, and Dipartimento di Scienze Chimiche, Università di Catania, and INSTM, UdR Catania, Viale A. Doria 6, 95125 Catania, Italy

Received March 14, 2007. Revised Manuscript Received June 29, 2007

Praseodymium aluminum oxide ($PrAlO_x$) thin films have been grown by metal organic chemical vapor deposition (MOCVD) using two different multimetal sources consisting of mixtures of aluminum acetylacetonate ($Al(acac)_3$) with two praseodymium precursors, namely, the praseodymium hexafluoroacetylacetonate diglyme adduct ($Pr(hfa)_3$·diglyme) and the praseodymium tetramethylheptanedionate ($Pr(tmhd)_3$). Smooth and amorphous films have been deposited on Si(100) substrates. Their chemical composition and microstructure, investigated by EDX measurements and TEM analyses, are deeply affected by the nature of the precursor mixture. Optimal structural and compositional properties are achieved with a $Al(acac)_3$−$Pr(hfa)_3$·diglyme mixture. Annealing procedures at 900 °C under an inert ambient atmospher do not affect the film crystallization. Preliminary electrical characterizations indicate a dielectric constant of about 12.

Introduction

Rare-earth aluminate thin films are currently used for a wide range of applications.[1−6] In the field of microelectronics, for instance, the integration of rare-earth-based aluminates onto semiconducting materials such as Si, SiC, GaAs, and GaN remains a challenging task for potential applications utilizing both information processing and data storage in the same device. In particular, the impressive development of complementary metal-oxide-semiconductor (CMOS) technology remains, to date, mostly associated with the important properties of the SiO_2−Si system.[1−4] Silicon oxide, the first dielectric material used in the MOS structures, still possesses numerous advantages,[7] although the unique drawback is associated with the rather low dielectric constant $\epsilon_R = 3.9$, which precludes any further decreasing in the device size.[8] The present CMOS technology requires a 4 nm SiO_2 gate dielectric layer,[9] and a further downsizing of the gate thickness is expected for the next-generation devices. Nowadays, dielectric layers as thin as 1.5 nm[10] can be reliably grown even though the further decrease in SiO_2 thickness remains a serious problem because of undesirable physical phenomena, such as tunneling between gate and channel.[11] The dispersion current density exponentially increases upon decreasing the oxide thickness[8] and is responsible for the high-energy consumption and heat generation with a consequent degradation of device performances.

Problems associated with the "scaling-down" of the physical thickness of the gate insulators[12] can be solved by adopting alternative layers of new dielectric materials having higher dielectric constant values. Thus, all the materials possessing dielectric constant values higher than $\epsilon_{SiO_2} = 3.9$ are defined as "high-*k* dielectrics".

Recently, great attention has been devoted to the praseodymium oxide, Pr_2O_3. It possesses a high dielectric constant value (about 26−30) that reduces the leakage current density, a high formation energy (−12900 kJ/mol), and a wide band gap of about 3.9 eV.[13,14] Pr_2O_3 films deposited by the MOCVD technique[15−19] have shown high dielectric constant

* Corresponding author. E-mail: raffaella.lonigro@imm.cnr.it (R.L.N.) or gmalandrino@dipchi.unict.it (G.M.).
† IMM-CNR.
‡ Università di Catania.

(1) Frosch, C. J.; Derick, L. *Proc. Electrochem. Soc.* **1957**.
(2) Ligenza, J. R.; Spitzer, W. G. *J. Phys. Chem.* **1961**, *65*, 2011.
(3) Ligenza, J. R.; Spitzer, W. G. *J. Phys. Chem. Solids* **1960**, *14*, 131.
(4) Gibaudo, G.; Clerc, R.; Vincent, E.; Bruyere, S.; Autran, J. L. *C. R. Acad. Sci. Paris* **2000**, *IV*, 911.
(5) Feofilov, S. P.; Kaplyanskii, A. A.; Zakharchenya, R. I. *J. Lumin.* **1997**, *72*, 41.
(6) Feofilov, S. P.; Kaplyanskii, A. A.; Kulinkin, A. B.; Kutsenko, A. B.; Vasilevskaya, T. N.; Zakharchenya, R. I. *Radiat. Eff. Defects Solids* **1999**, *151*, 943.
(7) Green, M. L.; Sorsch, T. W.; Timp, G. L.; Muller, D. A.; Weir, B. E.; Silverman, P. J.; Moccio, S. V.; Kim, Y. O. *Microelectron. Eng.* **1999**, 48.
(8) Buchanan, D. A. *IBM J. Res. Dev.* **1999**, *43*, 3.
(9) Fischetti, M. V.; Laux, S. E. *Appl. Phys. Lett.* **2000**, *76*, 2277.
(10) Mussig, H. J.; Dabrowsky, J.; Ignatovich, K.; Liu, J. P.; Zavodinsky, V.; Osten, H. J. *Surf. Sci.* **2002**, *504*, 159.
(11) Gusev, E. P.; Cartier, E.; Buchanan, D. A.; Gribelyuk, M.; Copel, M.; Okorn-Schimdt, H.; D'Emic, C. *Microelectron. Eng.* **2001**, *59*, 341.
(12) Lysaght, P. S.; Chen, P. J.; Bergamann, R.; Messina, T.; Murto, R. W.; Huff, H. R. *J. Non-Cryst. Solids* **2002**, *303*, 54.
(13) Osten, H. J.; Liu, J. P.; Bugiel, E.; Mussig, H. J.; Zaumseil, P. *Microelectron. Reliab.* **2001**, *41*, 991.
(14) Osten, H. J.; Liu, J. P.; Bugiel, E.; Mussig, H. J.; Zaumseil, P. *J. Cryst. Growth* **2002**, *235*, 229.
(15) Lo Nigro, R.; Raineri, V.; Bongiorno, C.; Toro, R.; Malandrino, G.; Fragalà, I. L. *Appl. Phys. Lett.* **2003**, *83*, 129.
(16) Lo Nigro, R.; Toro, R.; Malandrino, G.; Raineri, V.; Fragalà, I. L. *Adv. Mater.* **2003**, *15*, 1071.
(17) Lo Nigro, R.; Toro, R. G.; Malandrino, G.; Condorelli, G. G.; Raineri, V.; Fragalà, I. L. *Adv. Funct. Mater.* **2005**, *15*, 838.

10.1021/cm070706t CCC: $37.00 © 2007 American Chemical Society
Published on Web 08/07/2007

values and low leakage current densities, and overall, they have shown interesting electrical properties that render them potentially useful for microelectronics applications.[20,21]

Despite it now being clear that polycrystalline Pr_2O_3 films show good dielectric properties, practical applications require amorphous films that possess a very high crystallization temperature and hence a great thermal stability during the thermal treatments required for MOS fabrication processes. Grain boundaries, in fact, are responsible for the appearance of preferential paths for electrical current, thus favoring the degradation of device performances.

In this context, great attention has been recently devoted to the synthesis of mixed-oxide systems containing Al_2O_3. In fact, it is well-known that aluminum oxide thin films on silicon substrate remain amorphous at temperatures as high as 1000 °C.[22] Moreover, it possesses an oxygen diffusion coefficient lower than that of the large majority of binary oxides.[23] This property precludes the oxygen diffusion toward the silicon substrate surface, thus avoiding the uncontrolled formation of a low-k SiO_2 layer at the interface. Finally, Al_2O_3 dielectric possesses a wider band gap (8.8 eV) than that of the Pr_2O_3, and a high "band offset" with respect to the silicon substrate. These properties are both very important in order to reduce problems related to leakage current density.

In this context, huge efforts are nowadays devoted to the fabrication of multicomponent MAl_xO_y (M = transition or rare earth ion metal) systems having high dielectric constants and good chemical stability on silicon substrate. Recently, studies on $HfAl_xO_y$ and $ZrAl_xO_y$ have demonstrated that these materials have interesting dielectric properties.[24,25]

In the present paper, we report on the first MOCVD synthesis of mixed $PrAlO_x$ system deposited on Si(100) substrate. In particular, it has been demonstrated that $PrAlO_x$ films can be grown using two different Pr−Al precursor mixtures. These sources consist of the Al(acac)$_3$ precursor mixed with the Pr(tmhd)$_3$ β-diketonate or alternatively with the Pr(hfa)$_3$•diglyme adduct (H-acac = 2,4-pentandione; H-hfa = 1,1,1,5,5,5-hexafluoro-2,4-pentandione; H-tmhd = 2,2,6,6-tetramethyl-3,5-heptandione; diglyme=$CH_3O(CH_2CH_2O)_2CH_3$)). Thermal stabilities and transport properties of both sources have been compared using thermogravimetric measurements. It will be shown that the Al(acac)$_3$−Pr(hfa)$_3$•diglyme mixture has better thermal properties that parallel the higher quality of the deposited films.

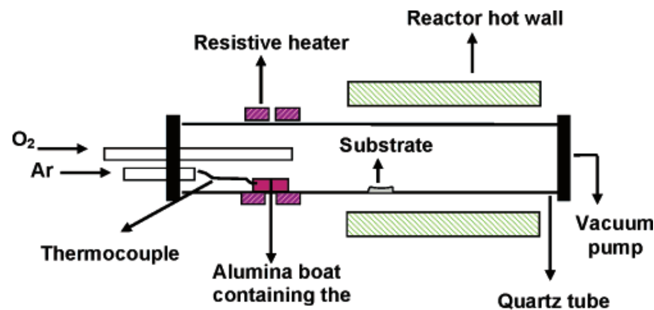

Figure 1. MOCVD hot-wall reactor scheme.

Experimental Section

Al(acac)$_3$ and Pr(tmhd)$_3$ complexes were purchased from Aldrich and used without further purification. The Pr(hfa)$_3$•diglyme was synthesized as described elsewhere.[26]

Thermogravimetric (TG) measurements were made using a Mettler Toledo TGA/SDTA 851[e]. Differential scanning calorimetry (DSC) was measured using a TC 10 processor and a DSC 30 calorimeter. The weight of the samples investigated was between 8 and 12 mg (TG) and 4 and 7 mg (DSC). Analyses were made under prepurified nitrogen using a 5 °C/min heating rate. Temperature was measured with an accuracy of ±0.1 °C.

A horizontal hot-wall, low-pressure MOCVD reactor 400 mm long and with a 28 mm diameter was used for growth experiments. The samples were positioned at 100 mm from the entrance (see Figure 1). The Pr−Al metallorganic sources consisted of finely mixed Pr(tmhd)$_3$ or Pr(hfa)$_3$•diglyme with the Al(acac)$_3$ complex. The precursor vaporization temperature was 120 and 160 °C for the Al(acac)$_3$−Pr(hfa)$_3$•diglyme and the Al(acac)$_3$−Pr(thmd)$_3$ mixtures, respectively. The vaporized source materials were transported by a 100 sccm argon gas flow to the deposition zone. Water-saturated oxygen flow (100 sccm) was used as reaction gas to avoid any F contamination. Depositions were carried out for 60 min at a 450 °C deposition temperature. The total pressure in the reactor chamber was about 79.8 Pa. All the experiences were performed on n-type (100) silicon substrates. They were cleaned ultrasonically using acetone, methanol, and isopropanol, and then etched in a 3% HF solution for 5 min to remove the native oxide and produce a hydrogen-passivated silicon surface.

Dielectric thin films were studied by X-ray diffraction (XRD). $\theta-2\theta$ XRD patterns were recorded in a grazing incidence mode (angle of incidence 1°), on a Bruker-AXS D5005 $\theta-\theta$ diffractometer, using a Göebel mirror to parallel the Cu Kα radiation operating at 40 kV and 30 mA. Film surface morphologies were examined using a Leo Iridium 1450 scanning electron microscope. The deposited films were also investigated by transmission electron microscopy (TEM: JEOL 2010 F, equipped with the Gatan imaging filter, instruments). Film atomic composition was determined by energy-dispersive X-ray analysis (EDX) using an Oxford solid-state detector, which produces analyses with errors of 8% for light elements and 4% for heavy ones. X-ray photoelectron analysis (XPS) has been performed using a PHI ESCA/SAM 5600 Multy technique spectrometer. XPS experiments were carried out with a base pressure of 2.6×10^{-8} Pa. A monochromated Al Kα radiation source ($h\nu = 1486.6$ eV) was used and XPS spectra were collected at various photoelectron angles (relative to the sample surface) in

(18) Lo Nigro, R.; Malandrino, G.; Toro, R. G.; Fragalà, I. L. *Chem. Vap. Dep.* **2006**, *12*, 109.
(19) Lo Nigro, R.; Malandrino, G.; Toro, R. G.; Fragalà, I. L *Topics in Applied Physics: Rare Earth Oxide Thin Films—Growth, Characterization and Applications*; Springer, NY, 2007; Vol. 106, p 33.
(20) Fiorenza, P.; Lo Nigro, R.; Raineri, V.; Lombardo, S.; Toro, R. G.; Malandrino, G.; Fragalà, I. L. *Appl. Phys. Lett.* **2005**, *87*, 231913/1.
(21) Fiorenza, P.; Lo Nigro, R.; Raineri, V.; Lombardo, S.; Toro, R. G.; Malandrino, G.; Fragalà, I. L. *J Appl. Phys.* **2005**, *98*, 044312/1.
(22) a) Chin, A.; Liao, C. C.; Lu, C. H.; Chen, W. J.; Tsai, C. *2001 Symposium on VLSI Circuits*: *Digest of Technical Papers*; Institute of Electrical and Electronic Engineers: New York, 2001; p 135. (b) Kim, W. S.; Kawahara, T.; Itoh, H.; Horiuchi, A.; Muto, A.; Maeda, T.; Mitsuhashi, R.; Torii, K.; Kitajima, H. *Jpn, J. Appl. Phys.*, Part I, **2004**, *43*, 1860. (c) Fujtsuka, R.; Sakashita, M.; Sakai, A.; Ogawa, M.; Zaima, S.; Yasuda, Y. *Jpn, J. Appl. Phys., Part I* **2005**, *44*, 2428.
(23) Green, M. L; Gusev, E. P.; Degraeve, R.; Garfuenkel, E. L. *Appl. Phys. Lett.* **2001**, *90*, 2057.
(24) Zhu, W.; Ma, T. P.; Tamagawa, T.; Di, Y.; Kim, J.; Carruthers, R.; Gibson, M.; Furukawa, T. *Tech. Dig.—Int. Electron Devices Meet*. **2001**, 464.
(25) Van Dover, R. B.; Lang, D. V.; Green, M. L.; Manchanda, L. *J. Vac. Sci. Technol. A* **2001**, *19*, 2779.
(26) Lo Nigro, R.; Toro, R.; Malandrino, G.; Fragalà, I. L.; Rossi, P.; Dapporto, P. *J. Electrochem. Soc.* **2004**, *151*, F206.

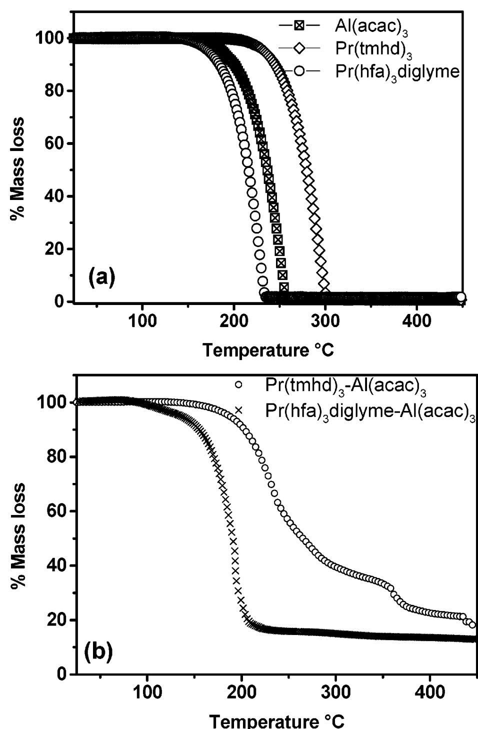

Figure 2. (a) TG curves of the $Pr(tmhd)_3$, $Pr(hfa)_3$•diglyme, and $Al(acac)_3$ precursors; (b) TG curves of the $Pr(tmhd)_3/Al(acac)_3$ and the $Pr(hfa)_3$•diglyme/$Al(acac)_3$ mixtures.

the 20−45° range. Depth profiles were obtained by alternating sputter etching rastered over a 4 × 4 mm^2 area (with a 4 kV argon ion gun) and XPS analysis. Au-gate MOS capacitors with an active area ranging from 7.85×10^{-5} cm^2 to 9.07×10^{-4} cm^2 were fabricated on n-type (100) Si substrate (5 mΩ cm^{-1}) with a p-type epi-layer of 20 Ω cm^{-1}. Capacitance−voltage ($C-V$) characteristics were measured at 1 MHz in a low noise probe station using a $C-V$ plotter (HP4284A).

Results and Discussion

Thermal Analysis. The present MOCVD process relies upon a novel approach based on the use of multicomponent "single" sources. To fully characterize the thermal behavior of the two mixtures, $Pr(tmhd)_3$−$Al(acac)_3$ and $Pr(hfa)_3$•diglyme−$Al(acac)_3$, we have carried out thermogravimetric analyses at atmospheric pressure under nitrogen flow of each single precursor, namely, $Al(acac)_3$, $Pr(tmhd)_3$,and $Pr(hfa)_3$•diglyme, and the two Pr−Al mixtures.

TG data (Figure 2a) show that the second generation $Pr(hfa)_3$•diglyme adduct is thermally stable and evaporates quantitatively in a single step in the 150−240 °C range with a residue left at 450 °C lower than 2%. The TG curve of $Al(acac)_3$ shows a single step that may be associated with sublimation without any decomposition process. In particular, its sublimation begins at 210 °C and ends at 260 °C, with a residue of about 2% at 400 °C. The TG profile of the $Pr(tmhd)_3$ precursor confirms its thermal stability and indicates that it vaporizes in the 240−310 °C range with a residue left at 450 °C of about 3−4%. It is possible to conclude that all the investigated precursors possess good thermal stability, because they sublime/evaporate in a single step with a low residue, and among them the second generation $Pr(hfa)_3$•diglyme adduct has the highest volatility.

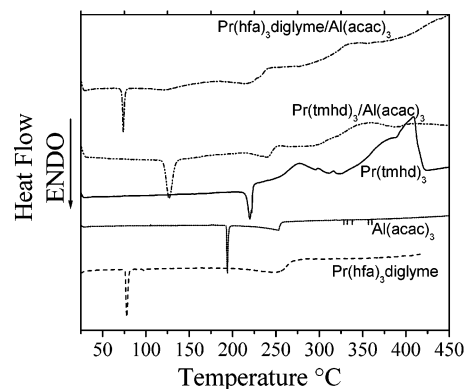

Figure 3. DSC curves of the single $Pr(hfa)_3$•diglyme, $Pr(tmhd)_3$, and $Al(acac)_3$ precursors and the multicomponent $Pr(tmhd)_3/Al(acac)_3$ and $Pr(hfa)_3$•diglyme/$Al(acac)_3$ mixtures.

In Figure 2b, the TG curves of the $Pr(tmhd)_3$−$Al(acac)_3$ and $Pr(hfa)_3$•diglyme−$Al(acac)_3$ mixtures (both having a 1:1 Pr:Al ratio) are compared. It becomes evident that the molten $Pr(hfa)_3$•diglyme−$Al(acac)_3$ mixture is more volatile than that containing the $Pr(tmhd)_3$ complex. In fact, the $Pr(tmhd)_3$−$Al(acac)_3$ mixture does not show a clean sublimation process, because two not very well defined steps are visible in the 200−400 °C temperature range with a large amount of residue left (18%) at 450 °C. A different behavior has been found in the case of the $Pr(hfa)_3$diglyme−$Al(acac)_3$ mixture, which evaporates in a single step in a narrower temperature range (150−230 °C) with a smaller amount residue (10%) left at 450 °C (Figure 2 b). Thus, in this case, both the Pr and Al precursors evaporate simultaneously with a clean process without any side decomposition.

The better thermal properties of the $Pr(hfa)_3$•diglyme−$Al(acac)_3$ mixture can be rationalized considering the low melting point (77 °C) of the second-generation Pr-$(hfa)_3$•diglyme precursor compared with that (220 °C) of the $Pr(tmhd)_3$ complex, as can be observed in the DSC curves of the two individual Pr precursors showing two sharp endothermic peaks at the temperature values reported above (Figure 3). The differential scanning calorimetry (DSC) curve of the $Al(acac)_3$ precursor (Figure 3) shows a sharp endothermic peak at 198.6 °C that is associated with melting of the Al precursor. The behavior of the two multicomponent sources is quite interesting. The $Pr(hfa)_3$•diglyme−$Al(acac)_3$ mixture curve shows a lower temperature peak (74 °C) that may be associated with melting of the $Pr(hfa)_3$•diglyme component. The small intensity feature in the 100−140 °C range represents dissolution of the second component in the molten Pr precursor, whereas the broad higher-temperature feature (170−225 °C) is possibly associated with the evaporation process. Nevertheless, the most intriguing issue of the mixture DSC curve is the absence of the endothermic peak at 198.6 °C expected for melting of the $Al(acac)_3$ precursor. Therefore, the $Pr(hfa)_3$diglyme adduct acts, on melting, as a solvent for the aluminum precursor, thus forming a single homogeneous molten mixture containing both the Pr and Al source.

By contrast, the curve of the $Pr(tmhd)_3$−$Al(acac)_3$ mixture shows a novel endothermic peak at 126.4 °C which accounts neither for the $Pr(tmhd)_3$ or the $Al(acac)_3$ melting points. This value is very close to the melting observed with

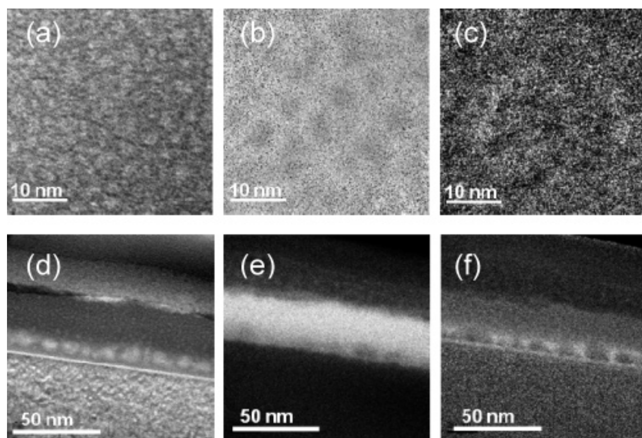

Figure 4. TEM images of a PrAlO$_x$ film deposited on Si (100) from the Pr(tmhd)$_3$−Al(acac)$_3$ mixture: (a) plan view; (b) EF-TEM Pr plan map; (c) EF-TEM Al plan map; (d) cross-section view; (e) EF-TEM Pr cross-section map; (f) EF-TEM Al cross-section map.

decomposition at 130 °C for the Pr(acac)$_3$ complex, and thus the presence of this peak seems to indicate a ligand exchange between Pr(tmhd)$_3$ and Al(acac)$_3$. Nevertheless, the possibility that the peak at 126.4 °C is the melting of an eutectic mixture in the binary Pr(tmhd)$_3$−Al(acac)$_3$ system cannot be excluded.

In conclusion, in the Pr(tmhd)$_3$−Al(acac)$_3$ mixture, each single precursor vaporizes quite separately, whereas the Pr(hfa)$_3$•diglyme−Al(acac)$_3$ mixture demonstrates great advantages for practical applications in depositing Pr−Al-containing films.

MOCVD from the Pr(tmhd)$_3$−Al(acac)$_3$ Mixture. In a series of experiments, the Pr(tmhd)$_3$−Al(acac)$_3$ mixture, in a 1:1 ratio, has been heated at 160 °C on the basis of the thermogravimetric studies. Films have been deposited on Si(100) substrates at 450 °C. The XRD pattern indicates that PrAlO$_x$ films are amorphous. An insight on the structural and compositional characterization of the deposited films has been obtained by transmission electron microscope (TEM). A plan TEM image (Figure 4a) shows a typical amorphous morphology. The chemical composition characterization has been carried out by energy-filtered TEM analyses, which produces elemental chemical maps employing electron energy losses. Energy-filtered chemical maps have been obtained using the typical elemental energy loss edge, which has been recorded with a postedge and two preedge windows to eliminate the environment and background signals. This represents an innovative technique to study chemical composition and the film−substrate interface by recording bidimensional chemical maps with high spatial resolution and sensitivity. In images b and c of Figure 4, the Pr and Al chemical bidimensional maps indicate that they are homogeneously distributed all over the entire surface. The quantification of the Pr:Al ratio has been performed by EDX in TEM mode. The EDX analysis revealed that the Pr:Al ratio is 0.85:0.15 and not the expected 1:1 as in the source mixture. Thus, the element distribution along the film thickness has been evaluated through TEM cross-section investigations. The TEM cross-section image (Figure 4d) showed that films consist of two deposited layers showing a different contrast. EF-TEM analyses performed along the entire film thickness indicate that the different contrast is due to the formation of two separate layers with different chemical compositions. In particular, the bottom brighter layer mainly consists of aluminum oxide, whereas the top darker layer is praseodymium-rich. The EDX analyses have shown that the bright bottom layer consists of an 80% Al−20% Pr layer, whereas the darker top layer contains a 15% Al−85% Pr mixture.

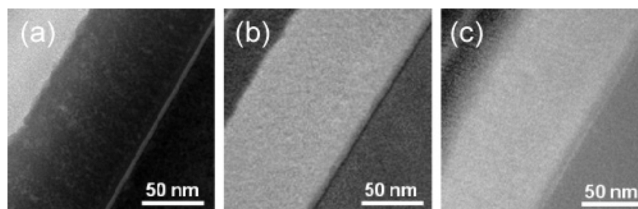

Figure 5. TEM images of a PrAlO$_x$ film deposited on Si(100) from the Pr(hfa)$_3$•diglyme−Al(acac)$_3$ mixture: (a) cross-section view; (b) EF-TEM Al cross-section map; (c) EF-TEM Pr cross-section map.

Therefore, the Pr(tmhd)$_3$−Al(acac)$_3$ mixture yields Pr−Al films with a chemical gradient from the interface toward the surface, giving rise to two different layers. These results may be explained considering that the Pr(tmhd)$_3$−Al(acac)$_3$ mixture does not allow us to control the different sublimation rates of the two precursors and causes the variation of chemical composition along the film thickness. In fact, the Al precursor is more volatile, and thus it is likely that at the beginning of the deposition source, vapors are richer in Al. During the film growth, the source vapors become progressively poorer in Al precursor and the resulting top layer mainly consists of Pr oxide. It cannot be excluded that if the two precursors are sublimed separately (e.g., at different temperatures), the use of these precursors may give rise to homogeneous films.

MOCVD from Pr(hfa)$_3$•diglyme−Al(acac)$_3$ Mixture. On the basis of previous studies[27−30] on the deposition of LaAlO$_3$ and YAlO$_3$ from multicomponent mixtures, where the second-generation fluorinated precursor acts as a solvent for the Al source, the potentiality of the Pr(hfa)$_3$•diglyme adduct to behave in a similar fashion and thus to deposit homogeneous PrAlO$_x$ films has been tested. Depositions have been carried out on Si (100) substrate at 450 °C in order to obtain amorphous films as required for microelectronics applications. The Pr(hfa)$_3$•diglyme and Al(acac)$_3$ complexes have been mixed in a 1:1 ratio, and the mixture has been heated at 120 °C.

XRD analyses demonstrated that the deposited films are amorphous, as observed for films deposited from the Pr(tmhd)$_3$−Al(acac)$_3$ mixture. By contrast, in the present case, the EDX analysis in TEM mode of the layer indicates that the Pr/Al ratio is 1:1. Moreover, the TEM cross-section image indicates that the PrAlO$_x$ film possesses a uniform thickness, low roughness, and a good film−substrate interface (Figure 5a). Film thickness is much greater (70 nm) than that of films

(27) Malandrino, G.; Condorelli, G. G.; Lo Nigro, R. *Chem. Vap. Deposition* **2004**, *10*, 171.
(28) Malandrino, G.; Fragalà, I. L.; Scardi, P. *Chem. Mater.* **1998**, *10*, 3765.
(29) Malandrino, G.; Frassica, A.; Fragalà, I. L. *Chem. Vap. Deposition* **1997**, *3*, 306.
(30) Toro, R. G.; Malandrino, G.; Fragalà, I. L.; Keshu, W.; Leto, A.; Pezzotti, G. *J. Phys. Chem. B* **2006**, *110*, 23977.

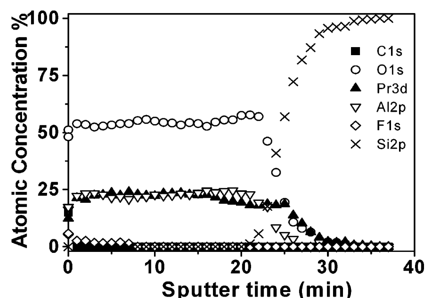

Figure 6. XPS depth profiles of a $PrAlO_x$ film deposited at 450 °C on Si(100) from the $Pr(hfa)_3$•diglyme−$Al(acac)_3$ mixture.

deposited from the $Pr(tmhd)_3/Al(acac)_3$ mixture (40 nm) using the same deposition time (60 min). These differences can be attributed to the higher volatility of the $Pr(hfa)_3$•diglyme−$Al(acac)_3$ mixture. However, the most significant data are that no evidence of compositional variation is visible. In fact, the Pr and Al EF-TEM maps (images b and c of Figure 5) showed a homogeneous distribution of both Pr and Al along the entire film thickness. The composition has been quantitatively determined by EDX analysis, which confirmed that the chemical composition is constant along the film thickness and that the Pr:Al ratio is 1:1.

Finally, carbon and fluorine contaminations have been excluded on the basis of XPS analysis results. The XPS profile (Figure 6) shows that the F1s signal decreases to zero after just one sputtering cycle. This trend is a clear evidence that no F contamination is present inside the deposited films. It is possible to conclude that the use of water-saturated O_2 flow as reaction gas was able to eliminate F contamination. Moreover, the C 1s signal is also zero after a few minutes of sputtering, thus indicating that the precursors cleanly decompose during the deposition process.

Note that also the XPS results confirm the Pr:Al ratio of 1:1 along the entire film thickness. These data indicate that the use of the $Pr(hfa)_3$•diglyme−$Al(acac)_3$ mixture together with the operational conditions allows a more precise control of the vaporization rate of both the Pr and Al sources, thus avoiding the formation of different layers.

One of the advantages of rare-earth oxide aluminates with respect to the pure rare-earth or transition metal oxides is the capability to remain amorphous after the high *T* treatment needed in the CMOS processing. Thus, the thermal stability of the deposited films from the $Pr(hfa)_3$•diglyme−$Al(acac)_3$ mixture has been studied by postdeposition annealing treatments at various temperatures in different atmospheres.

The annealing temperature has been varied from 800 to 900 °C and treatments have been performed in Ar and O_2 atmospheres. In oxygen ambient atmosphere, partial crystallization has been observed already at the lower (800 °C) annealing *T*, as shown in the TEM dark-field image (Figure 7), where very small crystalline grains are visible. By contrast, in inert ambient Ar atmosphere, films remain amorphous up to 900 °C.

Finally, preliminary electrical measurements have been performed in order to calculate the dielectric constant (ϵ)

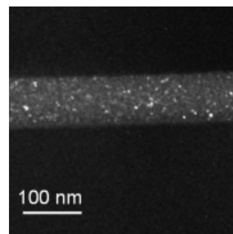

Figure 7. TEM dark-field image of a $PrAlO_x$ film deposited on Si(100) from the $Pr(hfa)_3$•diglyme−$Al(acac)_3$ mixture and annealed at 800 °C in ambient oxygen.

value. Capacitance−voltage measurements at 1 MHz on films 40 nm thick have demonstrated that the dielectric constant is about 12. Pr_2O_3 films having similar thickness possess dielectric constant values of 26, and thus the lower value presently found is probably due to the mixing between Pr oxides with the Al_2O_3 dielectric, which theoretically possesses $\epsilon \approx 9$.

Conclusions

Present results demonstrate the importance of the precursor behavior on the structural and compositional properties of the deposited $PrAlO_x$ films. Despite films have been deposited using the same operational parameters, relevant differences in the structural and compositional properties have been observed as a function of the precursor mixture. Films deposited from a $Pr(tmhd)_3$−$Al(acac)_3$ mixture consist of two separate layers: the bottom layer is Al-rich, whereas the top layer is Pr-rich. By contrast, films deposited from the $Pr(hfa)_3$•diglyme−$Al(acac)_3$ mixture are amorphous and homogeneous $PrAlO_x$ films. These films possess good thermal stability and interesting dielectric constant value.

These results can be explained considering the different behavior of the $Pr(tmhd)_3/Al(acac)_3$ and $Pr(hfa)_3$•diglyme/$Al(acac)_3$ mixtures. In fact, the low-melting (77 °C) $Pr(hfa)_3$•diglyme adduct acts as a solvent for the $Al(acac)_3$ complex, so that the present liquid mixture can be easily and cleanly evaporated from melt, thus providing constant mass-transport rates. On the contrary, the precursor mixture ($Pr(tmhd)_3$−$Al(acac)_3$) presents several drawbacks associated with thermal instability, sintering, and surface passivation upon sublimation, which in turn may render transport processes largely irreproducible.

Finally, the study of the MOCVD process presently reported represents an important step in the understanding of the deposition chemistry of mixed praseodymium−aluminum-based films. The low-cost and the simplicity of the adopted synthetic process make this approach of potential interest as a fabrication route to $PrAlO_x$ thin films.

Acknowledgment. The authors thank the INSTM (Consorzio Interuniversitario Nazionale per la Scienza e Tecnologia dei Materiali) for the financial support within the PRISMA project.

CM070706T